ADVANCED HEALTHCARE MATERIALS
www.advhealthmat.de

Investigation of Bone Regeneration Efficacy of New Bovine Bone Minerals in a Canine Mandibular Critical Defect Model

*Sung-Jin Park, Md. Mahbubur Rahman, Jaebum Lee, Suk-Woong Kang, and Sokho Kim**

This study aims to investigate the bone regeneration effect of bovine hydroxyapatite-processed biomaterials Bone-XB and S1-XB in a beagle mandibular defect model. A total of four saddle-type critical sizes (15 mm × 10 mm) bone defects are created in each dog: two defects in the left mandible and two defects in the right mandible. The defect control (DC) group is kept unfilled, and the other three defects are filled with three different biomaterials as follows: positive control Bio-Oss (Bio-Oss group), Bone-XB (XB group), and S1-XB (S1-XB group). Bone regeneration is evaluated by radiography, micro-computed tomography, and histological analysis. It is revealed that Bone-XB and S1-XB significantly increase newly formed bone, defect filling percentage, and bone healing score compared to the DC group, which is confirmed by bone microstructure augmentation (bone volume/total volume, trabecular number, and trabecular thickness). Interestingly, no significant differences are observed between the Bone-XB, S1-XB, and Bio-Oss groups. It is suggested that Bone-XB or S1-XB stimulates bone regeneration demonstrated by the increase in newly formed bone and bone microstructure, thereby improving bone defect filling, which is equivalent to the Bio-Oss. Therefore, bovine hydroxyapatite-processed Bone-XB or S1-XB can be considered effective biomaterials for correcting critical-size bone defects or fractures.

1. Introduction

Regenerative medicine for the regeneration of damaged tissues has made advances with the application of biomedical engineering in all applicable areas.[1–3] Among the diseases for which regenerative medicine can be applied, bone loss, fractures, and their resulting clinical management significantly impact health, social, and economic burdens. Over 20 million people worldwide are affected by bone tissue loss annually, and 5 million people require orthopedic surgical corrections, with 60% bone grafting to correct bone defect sites.[4]

Bone grafting is widely used in orthopedics for extensive bone defects in acute extremity fractures and delayed union and non-union after treatment. Furthermore, appropriate bone grafting is essential for various diseases and surgical procedures, such as spinal fusion, arthroplasty, osteomyelitis, and bone tumors. Although the bone graft material conditions should satisfy the effects of osteogenesis, osteoinduction, and osteoconduction. Autologous bone grafting is still considered the most useful bone graft among various bone grafting methods because of these three effects.[3,5] However, other bone graft methods should be considered since autograft has disadvantages, such as limited supply and donor site complications.

Allografts are also widely challenging to use because of disease transmission, the risk of infection, and immune response

S.-J. Park, M. M. Rahman, S. Kim
Research Center
HLB bioStep Co., Ltd.
Incheon 22014, Republic of Korea
E-mail: skim@hlbbiostep.com

S.-J. Park
Laboratory of Hygienic Pharmacy
College of Pharmacy
Chungbuk National University
Cheongju 28160, Republic of Korea

M. M. Rahman
Department of Physiology
College of Medicine
Gachon University
Incheon 21936, Republic of Korea

J. Lee
Medpark Co., Ltd.
Seoul 07282, Republic of Korea

J. Lee
Laboratory for Applied Periodontal & Craniofacial Research
Adams School of Dentistry
University of North Carolina
Chapel Hill, NC 27599, USA

S.-W. Kang
Department of Orthopedic surgery
Busan National University Yangsan Hospital
Yangsan 50612, Republic of Korea

The ORCID identification number(s) for the author(s) of this article can be found under https://doi.org/10.1002/adhm.202202942

DOI: 10.1002/adhm.202202942

problems. Therefore, porous bone mineral substitutes in orthopedics have recently increased. Furthermore, osteosynthesis can be induced in these bones through theoretical mechanisms.[5] In addition to these compositional components, morphological characteristics that promote bone healing and facilitate their application at the treatment site are also important. Notably, bone graft materials of powder, particle, chip, block, and gel types are used.[6] However, because the shape and size of the bone defects are different, it is difficult to apply them uniformly. Therefore, the importance of customized bone graft material has emerged because of the inconvenience and inapplicability of bone graft procedures.

Unlike long bone fractures, maxillofacial bone fractures occur due to automobile accidents, bicycle accidents, fall injuries, gunshot wounds, or various traumatic injuries.[7,8] Large defects usually occur in the maxillofacial bone following these injuries, whereas the mandible is mostly affected. The prevalence of facial fractures was reportedly 15% in the pediatric population and ≈8% in children aged 12 years.[8,9] Furthermore, extensive bone resections are required for correction when severe pathological conditions occur in skeletal diseases such as osteosarcoma, osteomalacia, osteoporosis, osteomyelitis, avascular necrosis, and congenital disabilities.[10] However, bone resections may also create critical bone defects. Adult periodontitis is the most common dental disease in the world. As periodontal disease progresses, alveolar bone loss can threaten systemic health due to decreased chewing ability and nutrient intake.[11] In addition, periodontal disease, tumor resection of the mandible, atrophy of the alveolar ridge following tooth loss, and congenital disabilities may necessitate mandibular reconstruction.[3,12]

Although physiologically, bone regenerates within 6–8 weeks following injury to restore its pre-injury status, bone substitutes are required in large bone fractures or defect repair.

Bone graft materials and membranes are commonly used in bone regeneration. Bone mineral grafts provide space and allow the growth of new bone, and the membrane contains the powdered bone graft material and preserves its shape.[6] For ideal bone formation, it is crucial to shape the bone graft material to the desired contour and maintain the createshape until the bone grows into the graft material. Currently, most of the existing bone graft materials in the market are powder-type bone minerals with poor shape retention.[13] Consequently, a titanium-reinforced membrane was introduced to preserve the shape of the graft. However, the application of membranes is a very technique-sensitive procedure that requires an advanced level of training. Therefore, an easily moldable bone graft material is what the market needs for the simple application of bone grafts. Recently, a bone graft material was developed to maintain its shape using various biocompatible additives.[6] This study used new moldable bone graft materials made of bovine hydroxyapatite-processed biomaterials, Bone-XB and S1-XB. Furthermore, Bio-Oss, which is widely used for bone regeneration, was used as a positive control for the comparative evaluation of equivalence.

Bone-XB is a bovine-derived bone graft material. Its pH is similar to that of body fluids, it has high blood permeability, and it enables rapid new bone formation without an inflammatory reaction. S1-XB is a natural bone graft material derived from bovine sources. Sticky bones can be created using saline alone without the need for blood. Bone-XB and S1-XB have similar physicochemical characteristics that represent high porosity, which promotes new bone formation due to advanced blood circulation. Furthermore, S1-XB has enforced osteoblast differentiation and cell adhesion due to the addition of bioactive substances that are distributed around the granule. The present study aimed to investigate whether a new bone graft material such as Bone-XB and S1-XB can maintain its shape and allow bone formation similar to the existing bone graft material, Bio-Oss.

2. Experimental Section

2.1. Bone Substitute

Two types of biomaterials, Bone-XB (Lot No.: XB200103P4001, MedPark Co., Ltd, Busan, Republic of Korea) and S1-XB (Lot No.: XBP191118P4001, MedPark Co., Ltd, Busan, Republic of Korea), were porous biocompatible bone grafts used in filling and augmentation of bony voids, periodontal, oral, and maxillofacial surgery. Both materials were provided as porous granules ≈0.2–1.0 mm in size. The first was made of natural bovine hydroxyapatite, removing organic components, and the latter was made of a mixture of natural bovine hydroxyapatite and biocompatible hydrogels. These biomaterials' efficacy was compared to that of another popular biomaterial, Bio-Oss (Geistlich Pharma AG, Wolhusen, Switzerland).

2.2. Animals and Management

In this study, 15 healthy mature male beagles (*Canis lupus familiaris*) dogs (40 weeks old; body weight 12.00–15.00 kg) were used, which were purchased from Saeronbio Inc. (Uiwang-si, Gyeonggi-do, Republic of Korea). They were housed separately in stainless steel cages (W 895 × L 795 × H 765 mm) in an environmentally controlled room (temperature: 23 ± 3 °C, relative humidity: 55 ± 15%, ventilation frequency: 10–20 times per h, light cycle: 8 am–8 pm, illumination: 150–300 Lux). Food and sterilized water were available ad libitum. Two-week acclimation period was maintained before the experimental procedures. All experimental protocols were approved by the committee on the Care of Laboratory Animal Resources, HLB bioStep, Korea (certificate number:20-KQ-003).

2.3. Teeth Extraction

After 8 h of fasting, the animals were anesthetized with a combination of Rompun (Bayer Korea, Seoul, Korea) and Zoletil (Virbac; Carros, France). Briefly, Zoletil (Tiletamine/zolazepam) powder (50 mg) and Rompun (Xylazine 2%, 5 mL) was mixed, and 0.1 mL kg^{-1} was injected intravenously. Isoflurane (0.5–5%) in O_2 (100%) was used to maintain anesthesia.[14] In addition, bupivacaine (0.5–1 mL) was injected locally into the inferior alveolar/mandible for local anesthesia before surgery. NaCl (0.9%) in saline (10 mL kg^{-1} h^{-1}) intravenously throughout the surgical procedure.[14] Cephalosporin (5 mg kg^{-1} IM) and tramadol (3 mg kg^{-1}, SC) were administered before surgery. The animal

was placed in left lateral recumbency, and scaling was performed before extraction. A surgical incision was made along the first premolar and the first molar to create a single gingival flap to the depth of the alveolar bone on the buccal aspect, followed by the use of freer elevators to complete the exposure of the alveolar bone. Subsequently, the crowns of the second, third, and fourth premolars were sectioned into two pieces and the first molar into three pieces owing to its three-rooted nature from the furcation via a high-speed burr. Subsequently, alveolotomy via a high-speed bur was performed to expose the periodontal ligament, and the sectioned crown/root segments were carefully extracted at the right site. Finally, the flap was closed without tension using synthetic monofilament absorbable suture material. Similarly, all procedures were performed on the left side to extract the first molar, first, second, third, and fourth premolar teeth. Cephalosporin and tramadol were continued seven days postoperatively. All animals were kept for eight weeks for extraction site recovery, and mandibular defects were created during the second surgery.

2.4. Critical Size Defects

The critical-size defect was selected following the study by Hunt et al.[15] Anesthesia and premedication for surgical preparation were administered in the first surgery. Subsequently, an incision was made to create a gingival flap on the buccal and lingual gingiva at the extraction site. Next, freer elevators were used to completely elevate the gingiva from the alveolar bone. To create a saddle-type defect, 15 mm mesiodistally × 10 mm apicocoronally lines were confirmed. Subsequently, a reciprocating mini saw was used to create the desired block, which was carefully removed from the alveolar bone using a luxator. Similarly, the second defect was made 10 mm away from the first defect on the same side. Therefore, four defects were created in each animal: two defects in the left mandible and two defects in the right mandible.

In each animal out of four defects, one defect was kept empty as the defect control group (DC), and the other three defects were filled with three different biomaterials: positive control group that were filled by Bio-Oss (Bio-Oss), Bone-XB-filled group (XB), and S1-XB-filled group (S1-XB). The filling graft materials were altered among sites in subsequent animals. Therefore, the total sample size for each group was 15. Considering the scientific sample number reported previously,[16] the fewest number of animals possible, consistent with the study objectives, was used.

Subsequently, the gingival flaps were closed, without tension, carefully using absorbable monofilament suture material. Following surgery, the surgical site was checked carefully once daily for three days and then once per week until the end of the experiment to confirm any abnormalities, such as signs of infection, inflammation, bleeding, or general integrity. The dogs were fed a soft diet for two weeks after the surgical procedure, and no abnormal signs or deaths were observed during the entire experimental period.

2.5. Sample Collection and Dental X-Ray

Following the second surgical procedure, the animals (five dogs in each group) were euthanized using potassium chloride (2 mEq kg^{-1}, IV) under general anesthesia at 4, 8, and 12 weeks. Bone defects of mandibles and 2 mm surrounding tissues, membrane, and adjacent hard tissue were harvested as a single unit for photography and radiography and then fixed in 10% neutral buffered formalin.

Radiographs were obtained using dental portable X-ray equipment (ADX4000, DEXCOWIN Co., Ltd., Seoul, Korea) to evaluate the degree of bone defect healing and interpreted by scoring methods (0–5) as described previously:[17] 0, no visible new bone formation; 1, minimal new disorganized bone; 2, disorganized new bone bridging graft to host at both ends; 3, organized new bone of cortical density bridging at both ends; 4, loss of graft-host distinction; and 5, significant new bone and graft remodeling.

2.6. Micro-Computed Tomography

Micro-computed tomography (CT) of the collected samples was performed using Scanco Viva CT 80 (Scanco Medical AG, Bassersdorf, Switzerland) according to the manufacturer's instructions. To quantify bone volume/total volume (BV/TV) [%], trabecular number (Tb.N) (1 mm), trabecular thickness (Tb.Th) (mm), and trabecular separation (Tb.Sp) (mm), samples were scanned at an isotropic voxel size of 40 µm (45 kVp energy, 177 µA intensity, 40 mm FOV/diameter, and 180 ms integration time). The selection of the scan energy and voxel size (scanning increment) was based on optimizing the scanning time and tissue detail and minimizing the exposure to radiation according to the manufacturer's instructions. Bone volume/total volume(BV/TV), Trabecular number(Td.N), Trabecular thickness(Tb.Th), Trabecular separation(Tb.Sp) had been evaluated. Each parameter was analyzed from the 3D reconstructions of the micro-CT scans generated by the imaging software (Evaluation program V6.6, SCANCO Medical, Swiss).

2.7. Histopathological Examination

A non-decalcification method was performed with Goldner's trichrome stain (for histomorphometry) and hematoxylin and eosin (H&E) staining (for histopathological examination). Six orofacial step sections of each block with a thickness of ≈200 µm were obtained using a diamond saw blade in the buccolingual plane. The sections were then polished to ≈50–80 µm using a special grinding machine. Three sections from each block (mesial, center, and distal) were stained using the H&E method, and the three remaining sections were stained by Goldner's trichrome method.

The area stained with Goldner's trichrome stain for histomorphometric examination was analyzed. Newly formed bone, residual material, fibrous tissue formation, existing bone, void space, and defect filling were evaluated using a modified technique, as previously described.[18] the rectangular area of interest (AOI) was defined as follows: 1) Apico-coronal (maximum size of the apico-coronal length in all samples; #9 Animal, Left Distal-second slide): 21 217.634 µm; 2) Mesio-distal (maximum mesio-distal length in all samples; #15 Animal, Right Mesial-first slide): 12 879.331 µm. The results were calculated using the following formula: Area of interest (μm^2) = 21 217.634 µm (maximum size

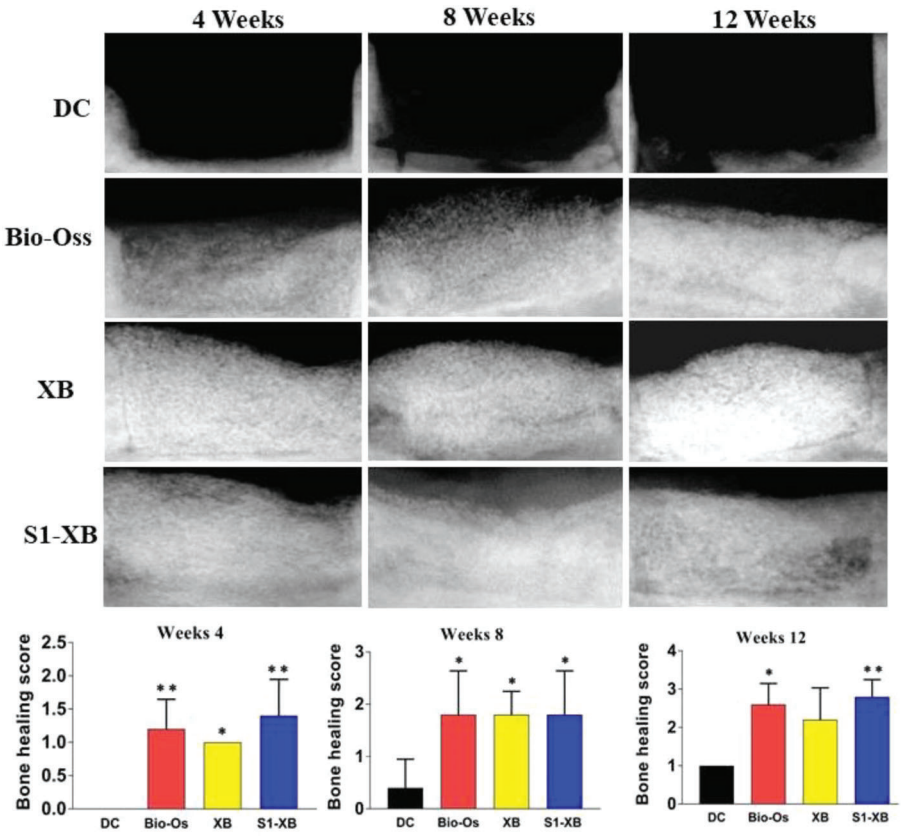

Figure 1. Radiographic evaluation of bone healing.

of apico-coronal length in all samples) ×12 879.331 μm (maximum size of mesiodistal length in all samples). The equal maximum size of the AOI in all samples was defined as apico-coronal and mesio-distal. In addition, an image analyzer (Zen 3.1, Carl Zeiss, Germany) was used for the histomorphometric examination. Lastly, defect filling was calculated as the sum of the newly formed bone, residual material, and fibrous tissue formation.

2.8. Statistical Analysis

The results were analyzed by parametric (One-way ANOVA) or non-parametric multiple comparison procedure (Kruskal–Wallis test). When the result of ANOVA was significant, Dunnett's multiple comparisons test (parametric) or Dunn's multiple comparisons test (non-parametric) were applied for the comparison between control group and test article administered group each necropsy points. All statistical analysis was performed using Prism 7.04 (GraphPad Software Inc., San Diego, CA, USA), and if p-value is <0.05, the result was considered statistically significant. Data were represented as mean ± standard deviation as applicable.

3. Results

3.1. Radiography Evaluation

The bone defect healing scores of the Bio-Oss, XB, and S1-XB groups were significantly higher ($p < 0.05$) than those of the DC group after 4, 8, and 12 weeks. However, no statistically significant differences between the bone defect healing scores of the Bio-Oss, XB, and S1-XB groups were observed ($p > 0.999$; **Figure 1**). Overall, in the Bio-Oss, XB, and S1-XB groups, it was observed that new bone formation started at 4th week, mineral bone bridge formation at 8th week, and bone bridge formation at both ends at 12th week.

Radiographs were obtained to evaluate the degree of bone defect healing and interpreted by scoring methods (0–5): 0, no visible new bone formation; 1, minimal new disorganized bone; 2, disorganized new bone bridging graft to host at both ends; 3, organized new bone of cortical density bridging at both ends; 4, loss of graft-host distinction; and 5, significant new bone and graft remodeling. Data are represented as means ± SD, $n = 5$, p-values are calculated using one-way ANOVA with Prism 7.04, $^{*}p < 0.05$, $^{**}p < 0.01$, and $^{***}p < 0.001$. Defect control group, DC; positive control group which were filled by Bio-Oss, Bio-Oss; Bone-XB-filled group, XB; S1-XB-filled group, S1-XB

3.2. Micro-Computed Tomography Evaluation

Bone regeneration was statistically significant in the treated groups at all time points of sample collection (4, 8, and 12 weeks) but insignificant in the DC group (**Figure 2**). The percentage of BV/TV in Bio-Oss, XB, and S1-XB groups was significantly higher than that of the DC group ($p < 0.05$) at all experimental sample collection time points (4, 8, and 12 weeks). There were no

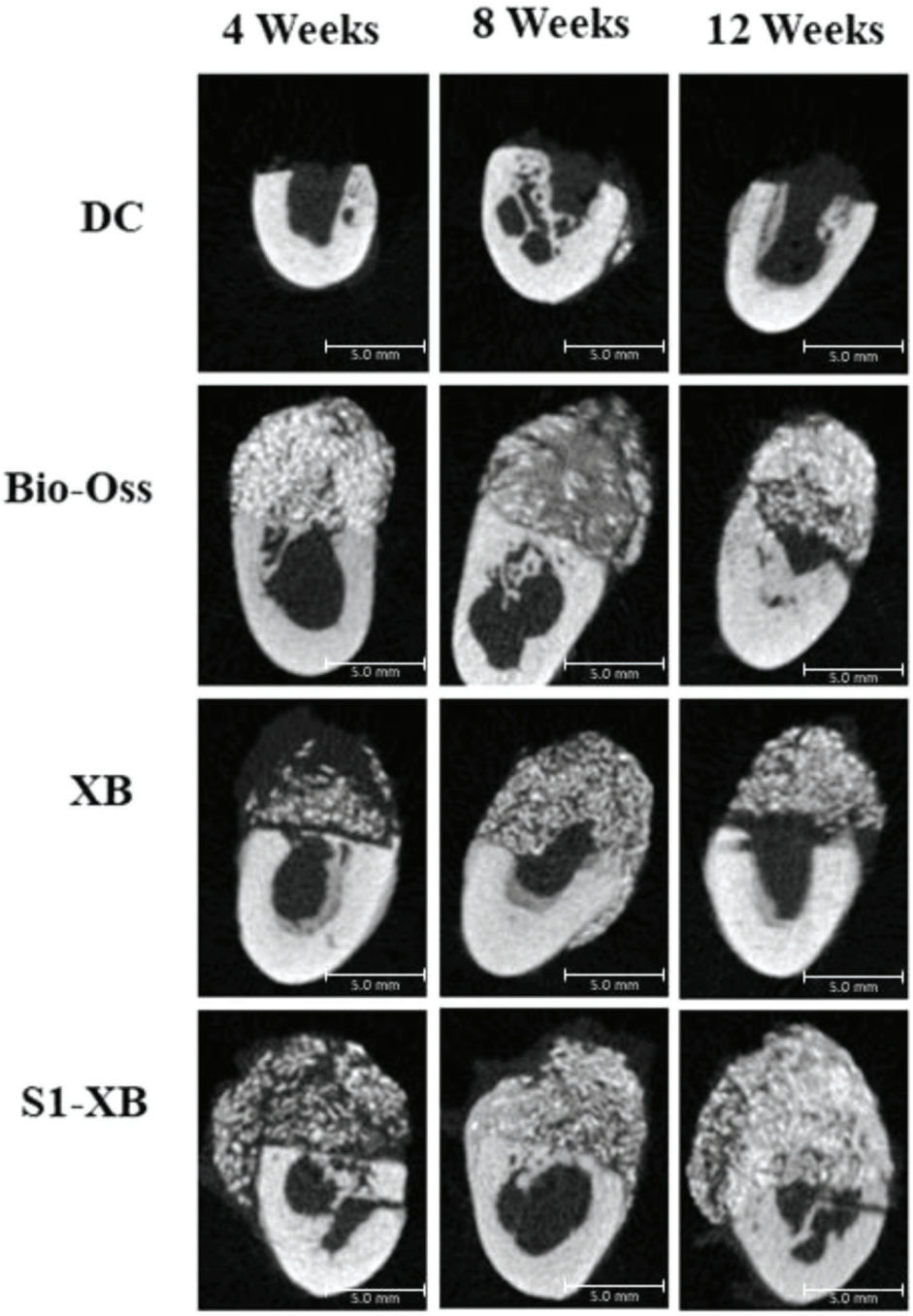

Figure 2. Representative micro-computed tomography showing bone formation after 4, 8, and 12 weeks healing.

statistically significant differences between the BV/TV levels of the Bio-Oss group and that of the XB and S1-XB groups ($p = 0.998$ and $p = 0.999$, respectively). The amounts of Tb.N and Tb.Th in the treated groups were also higher after 4 weeks but significantly higher after 8 and 12 weeks. In addition, the amount of Tb.Sp was significantly lower in all treated groups (Bio-Oss, XB, and S1-XB) after 4, 8, and 12 weeks (**Table 1**).

Calibration length is 5.0 mm. defect control group, DC; positive control group that were filled by Bio-Oss, Bio-Oss; Bone-XB-filled group, XB; S1-XB-filled group, S1-XB

3.3. Histopathological Examination Analysis

As shown in **Figure 3**, varying amounts of the defect filling effect with new bone formation were found in the defect after 4 weeks, which were characterized by more intense red staining. In addition, 12 weeks after surgery, there was a further significant increase in bone volume at the superior site ($p < 0.05$). Furthermore, newly formed bone, existing bone (%), residual material (%), and fibrous tissue formation histomorphometry were evaluated by Goldner's trichrome method. The defect filling

Table 1. Evaluation of bone healing by micro-computed tomography analysis. Measurements of BV/TV, Tb.N, Tb.Th, and Tb.Sp of mandible trabecular bone after 4, 8, and 12 weeks post-treatment. Data are represented as means ± SD, $n = 5$, p-values are calculated using one-way ANOVA with Prism 7.04, $^{*}p < 0.05$, $^{**}p < 0.01$, and $^{***}p < 0.001$. Bone volume/total volume, BV/TV; trabecular number, Tb.N; trabecular thickness, Tb.Th; trabecular separation, Tb.Sp; standard deviation, SD; defect control group, DC; positive control group which were filled by Bio-Oss, Bio-Oss; Bone-XB-filled group, XB; S1-XB-filled group, S1-XB.

		DC	Bio-Oss	XB	S1-XB
BV/TV [%]	Week 4	1.00 ± 0.01	39.21 ± 6.05*	37.75 ± 7.36*	40.40 ± 9.22*
	Week 8	2.05 ± 1.79	46.31 ± 8.89**	48.11 ± 10.91**	32.16 ± 4.10*
	Week 12	2.03 ± 0.82	40.08 ± 2.28**	32.37 ± 11.22*	47.62 ± 7.97***
Tb.N [1/mm]	Week 4	0.03 ± 0.00	0.34 ± 0.08	0.28 ± 0.06	0.37 ± 0.06
	Week 8	0.03 ± 0.02	0.28 ± 0.05***	0.22 ± 0.04**	0.22 ± 0.03**
	Week 12	0.03 ± 0.01	0.26 ± 0.03***	0.22 ± 0.05**	0.23 ± 0.03**
Tb.Th [mm]	Week 4	0.38 ± 0.00	1.37 ± 0.35	1.65 ± 0.45	1.15 ± 0.28
	Week 8	0.41 ± 0.15	1.69 ± 0.22**	2.03 ± 0.36***	1.49 ± 0.09*
	Week 12	0.59 ± 0.10	1.69 ± 0.25*	1.41 ± 0.31	2.15 ± 0.33**
Tb.Sp [mm]	Week 4	37.46 ± 0.11	2.28 ± 0.63***	2.64 ± 0.65***	1.79 ± 0.43***
	Week 8	145.28 ± 58.53	3.03 ± 1.60**	3.22 ± 1.54**	3.51 ± 0.73**
	Week 12	42.16 ± 9.95	2.47 ± 0.30***	4.45 ± 1.65***	2.57 ± 0.66***

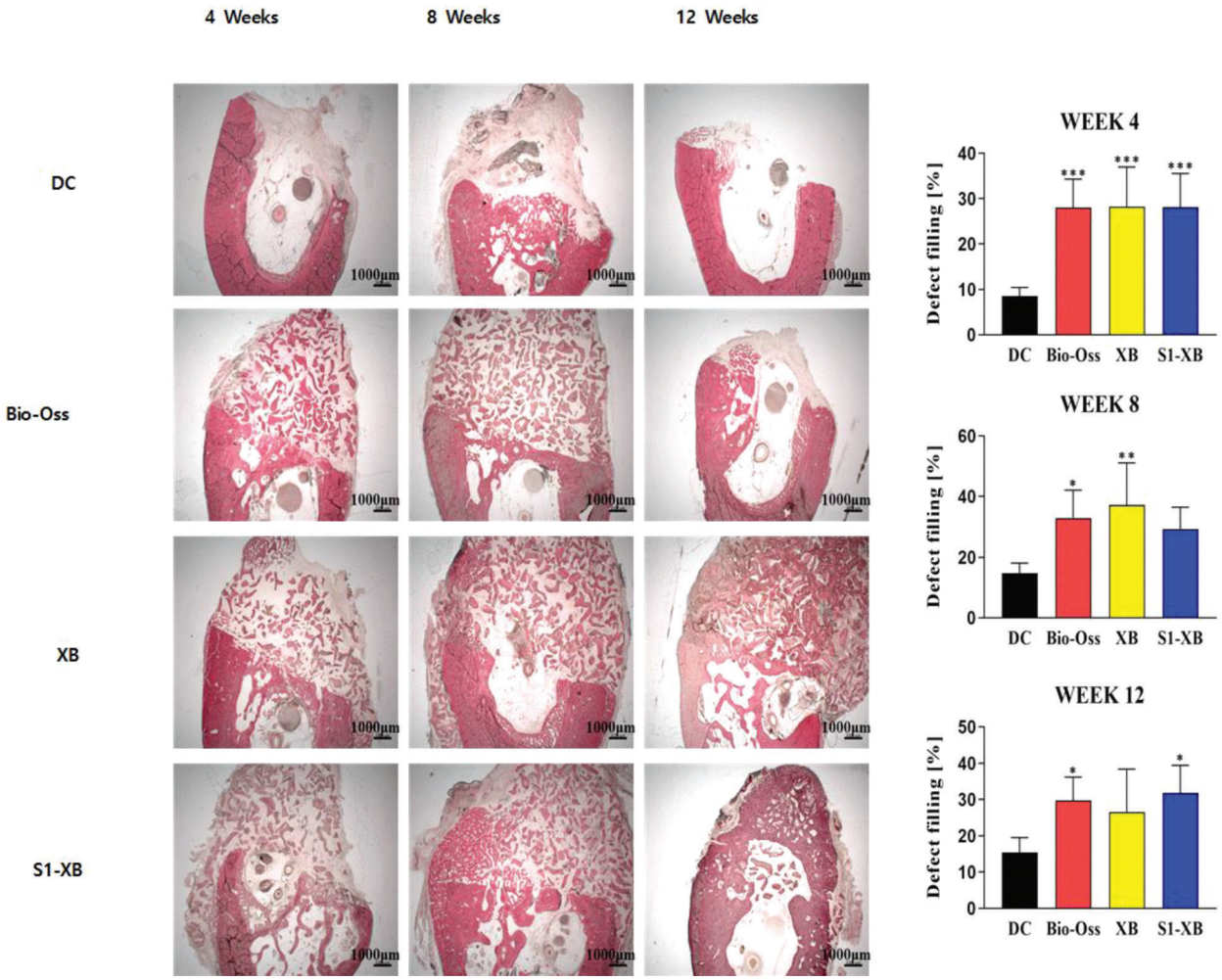

Figure 3. Evaluation of bone healing by histomorphometry analysis. All histopathological images are 10X magnification. Data are represented as means ± SD, $n = 5$, p-values are calculated using one-way ANOVA with Prism 7.04, $^{*}p < 0.05$, $^{**}p < 0.01$, and $^{***}p < 0.001$. defect control group, DC; positive control group which were filled by Bio-Oss, Bio-Oss; Bone-XB-filled group, XB; S1-XB-filled group, S1-XB.

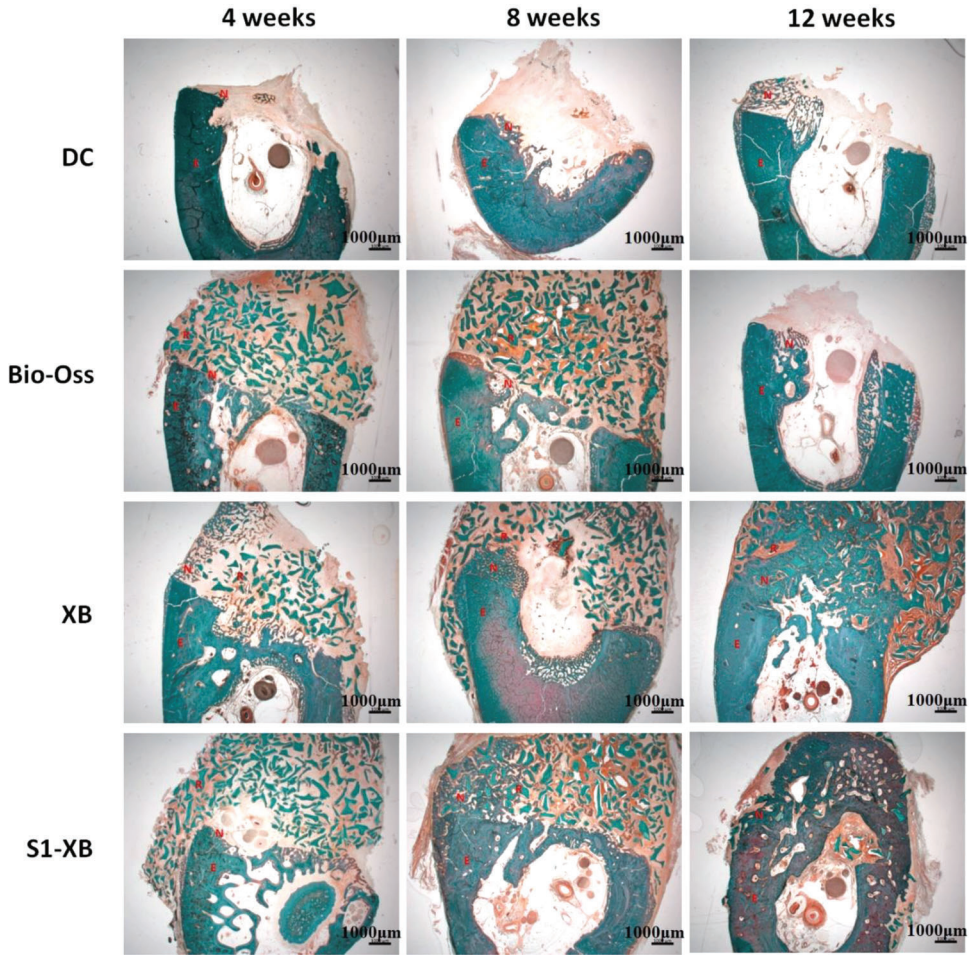

Figure 4. Evaluation of bone healing by Golder's trichrome stain histomorphometry analysis. All histopathological images are 10X magnification. defect control group, DC; positive control group which were filled by Bio-Oss, Bio-Oss; Bone-XB-filled group, XB; S1-XB-filled group, S1-XB. Newly formed bone, N; Existing bone, E; Residual material, R.

percentages were significantly higher in the Bio-Oss, XB, and S1-XB groups than in the DC group. Therefore, the Bio-Oss, XB, and S1-XB groups showed an improvement in bone defect healing and defect filling evaluated by histomorphometry compared to the DC group. In addition, the effect of improving bone defect healing and defect filling in the XB and S1-XB groups evaluated by histomorphometry did not show a significant difference compared to the Bio-Oss group (Figures 3 and **4** and **Table 2**), indicating similar bone regeneration effects. In these figures, we labeled 3 part of the region like newly formed bone as N, existing bone as E, and residual material as R. High magnification images (50× and 100×) are also confirmed in Figures S2 and S3 (Supporting Information).

4. Discussion

Canine bone and humans have several similarities, such as bone density, composition (bone organic, inorganic, and water fractions), weight, osteon remodeling activity, and epiphyseal fusion after maturity.[19] Therefore, preclinical bone healing studies on canine species are popular and scientifically accurate.[20–22] This study used a critical-size mandibular bone defect model in Beagle to investigate the bone regeneration effects of the Bone-XB and S1-XB biomaterials compared with Bio-Oss. It was observed that Bone-XB and S1-XB were therapeutically effective as Bio-Oss to regenerate bone in a known critical-size bone defect model, which was confirmed by radiography, micro-CT, and histopathological results.

A major surgical challenge in preclinical studies is developing critical-size bone defects due to physiological auto-regeneration. In addition, no specific research has confirmed the exact size of critical-size bone defects in canine mandibular defect models. However, some published articles are available for different sizes and types of defects in canine mandibular bone defect models. For example, bone defects of rectangular 10.0 × 5.0 × 5.0 mm in size, 7–10 mm mesiodistally, 6–8 mm apicocoronally, "'box-type,"' 4 × 5 mm (width × height), one wall intrabony, mesiodistal width: 5 mm × depth: 4 mm; buccolingual width: 3 mm, a circular, 8 mm wide bone defect.[20–24] Furthermore, a bone defect is considered a critical-size bone defect when new bone formation could not heal more than 10% during the animal's lifetime.[25] Huh et al. reported that ≈15 mm canine mandibular defects

Table 2. Evaluation of bone healing by Goldner's trichrome stain histomorphometry analysis. Data are represented as means ± SD, $n = 5$, p-values are calculated using one-way ANOVA with Prism 7.04, $^{*}p < 0.05$, $^{**}p < 0.01$, and $^{***}p < 0.001$. Defect control group, DC; positive control group that were filled by Bio-Oss, Bio-Oss; Bone-XB-filled group, XB; S1-XB-filled group, S1-XB.

		DC	Bio-Oss	XB	S1-XB
Newly formed bone [%]	Weeks 4	1.49 ± 0.49	3.66 ± 0.97	4.78 ± 1.24	3.22 ± 0.72
	Weeks 8	2.39 ± 0.41	5.99 ± 0.66	7.66 ± 2.07*	6.49 ± 1.15
	Weeks 12	2.69 ± 0.55	6.97 ± 0.78*	5.70 ± 1.08	7.31 ± 1.52*
Existing bone [%]	Weeks 4	11.18 ± 2.42	11.30 ± 1.84	12.72 ± 2.03	11.89 ± 0.94
	Weeks 8	12.57 ± 2.70	14.52 ± 2.36	12.90 ± 2.40	10.97 ± 1.52
	Weeks 12	10.73 ± 0.85	9.14 ± 1.21	8.58 ± 1.55	9.56 ± 0.73
Residual material [%]	Weeks 4	00 ± 0.00	5.14 ± 0.83**	4.47 ± 1.20*	4.44 ± 1.55*
	Weeks 8	00 ± 0.00	5.89 ± 1.09**	7.16 ± 1.63**	4.41 ± 1.40
	Weeks 12	00 ± 0.00	4.55 ± 0.23	3.82 ± 1.27	4.69 ± 1.18
Fibrous tissue formation [%]	Weeks 4	7.04 ± 1.09	19.22 ± 1.70**	18.95 ± 3.08**	20.45 ± 2.37**
	Weeks 8	12.37 ± 1.42	21.04 ± 3.07	22.37 ± 3.97	18.46 ± 3.15
	Weeks 12	12.78 ± 2.03	18.27 ± 2.74	19.96 ± 3.84	19.84 ± 2.03
Void space [%]	Weeks 4	0.16 ± 0.16	0.12 ± 0.07	0.09 ± 0.04	0.17 ± 0.04
	Weeks 8	0.12 ± 0.09	0.24 ± 0.07	0.16 ± 0.04	0.26 ± 0.11
	Weks 12	0.56 ± 0.30	0.01 ± 0.01	0.12 ± 0.12	0.19 ± 0.14
Defect filling [%]	Weeks 4	8.54 ± 0.84	28.02 ± 2.81***	28.20 ± 3.92***	28.11 ± 3.33***
	Weeks 8	14.77 ± 1.46	32.91 ± 4.11*	37.19 ± 6.23**	29.35 ± 3.22
	Weks 12	15.47 ± 1.82	29.79 ± 2.86*	26.47 ± 5.33	31.84 ± 3.39*

induced a limited new bone formation after 6 months of defect induction, though the bone defect/fracture healed within 6–8 weeks.[26] A 15 mm (length, mesiodistally) × 10 mm (depth, apicocoronally) saddle-type defect was selected as the critical size defect, and the body weight of the animals used in this study was approximately half the weight used in a previous study.[15] The study's relative mandibular bone defect size was larger than that reported by Hunt et al., and one site per animal was assigned as a negative control (DC group).[15]

In the present study, we confirmed whether new biomaterials such as Bone-XB and XB-S1 have potential ability of bone formation instead of Bio-Oss that is used for bone regeneration, commercially. Bio-Oss is a bone substitute material that is widely used in dental and orthopedic surgeries to support bone regeneration. It is composed of a natural mineral called hydroxyapatite, which is the main component of human bone. Geistlich Bio-Oss is crystalline hydroxyapatite with no detectable impurities referring to the product details. Its micromorphology is shown in Figure S1 (Supporting Information). Scanning electron microscope (SEM) images of test materials. Bone-XB is a bovine-derived bone graft material. Its pH is similar to that of body fluids, it has high blood permeability and enables rapid new bone formation without an inflammatory reaction. As a result of the porosimeter test, it was confirmed that it has a high porosity of 70% or more. The high porosity facilitates blood circulation and promotes new bone formation. Macro-pore and micro-pore were confirmed through SEM images (5000× images of Figure S1, Supporting Information) that promote the influx and differentiation of osteoblasts to increase new bone formation. S1-XB is a natural bone graft material also derived from bovine sources. Sticky bone can be created using saline solution alone without the need for blood collection. It has a sticky and moldable property that allows for shaping, and it has excellent fixation so that it does not scatter during irrigation. Bone-XB and S1-XB have similar physicochemical characteristics that represent high porosity, which promotes new bone formation due to advanced blood circulation. Macro-pore and micro-pore were also confirmed through SEM images (5000× images of Figure S1, Supporting Information). Furthermore, S1-XB is expected that enforced osteoblast differentiation and cell adhesion due to the addition of bioactive substances that are distributed around the granule (Figure S1, Supporting Information). It is strategically important to add special bioactive substances to increase the success potential of biomaterials.

It was observed that new bone formation started at 4th week, mineral bone bridge formation at 8th week, and bone bridge formation at both ends at 12th week in the Bio-Oss, XB, and S1-XB groups. In addition, 12 weeks after surgery, radiographic images showed that the bone healing score in the DC group was near "0". Consistently, defect filling in the DC group was significantly lower than in the treated groups. Therefore, it can be concluded that the mandibular bone defect in this study was critical-sized. In contrast, Bone-XB and S1-XB significantly increased the newly formed bone, defect filling percentage, and bone healing score compared to the DC group, which was further confirmed by bone microstructure augmentation. It was demonstrated that healing after implantation of our candidate materials was time-dependent, and that the bone bridge should recover for 12 weeks before implant placement.

Micro-CT imaging was performed to quantify bone regeneration since it accurately evaluates the bone quality and allows a 3D micro-architecture analysis of the bone.[21] This method can readily differentiate between newly formed and existing bone.[23,24] Moreover, bone structure and mass are necessary to evaluate bone quality.[21] The common parameters of cancellous bone are

BV/TV, Tb.N, Tb.Th, and Tb.Sp, which are the trabecular structural properties and micro-architectural properties of bone.[27] They reflect bone micro-volume, trabecular bone number, thickness, spacing, and trabecular network. Our results revealed the levels of BV/TV, Tb.N, and Tb.Th in Bone-XB and S1-XB were higher than in the DC group during the experimental periods (4, 8, and 12 weeks), whereas the Tb.Sp levels of Bio-Oss, Bone-XB, and S1-XB groups were lower than those in the DC group. According to the radiography results, micro-CT showed that Bio-Oss, Bone-XB, and S1-XB implants improved bone microstructure components in the defect sites compared to the DC group.

Histopathological examination by H&E staining was performed, and the results support the previous observations that the Bone-XB and S1-XB implants significantly increased the defect filling compared with the DC group. In addition, Golder's trichrome staining was further performed to confirm histomorphometric changes. Goldner's trichrome is an excellent stain for identifying cellular components and differentiating newly formed bone matrices from mature ones and calcified cartilage.[28] The results of this staining method further confirmed that Bone-XB and S1-XB significantly improved newly formed bone and defect filling percentages compared with the DC group and were similar to those of the Bio-Oss group.

In this experiment, the powder- and dough-type bones produced similar results; however, this may be because both walls of the saddle defect support the surgical site. Moreover, the dough-type bone was much easier to form during application surgery and maintained good shape after surgery. Therefore, dough-type S1-XB may be a suitable graft material for defects with insufficient surrounding support.

5. Conclusion

In summary, the results of radiography, micro-CT, and histological analysis showed that Bone-XB or S1-XB effectively regenerated bone, indicated by the increase in newly formed bone and bone microstructure (BV/TV, Tb.N, and Tb.Th), thereby improving bone defect filling in the beagle mandibular critical defect model and equivalent to the Bio-Oss. Therefore, the bovine-derived biomaterial Bone-XB or S1-XB could be considered an effective biomaterial for correcting critical-size bone defects or fractures in the mandible and large bone defects.

Supporting Information

Supporting Information is available from the Wiley Online Library or from the author.

Acknowledgements

The authors acknowledge the facilities and scientific, and funding assistance of HLB bioStep, MedPark, University of North Carolina, Busan National University, Gachon University and Chungbuk National University. The authors would like to express gratitude to all the staff who assisted with experiments and publication of this study. All experimental protocols were approved by the Committee on the Care of Laboratory Animal Resources, HLB bioStep, Korea, (Certificate number: 20-KQ-003).

Conflict of Interest

The authors declare no conflict of interest.

Author Contributions

S.-J.P. performed conceptualization, methodology, writing-original draft. M.M.R. performed software, formal analysis, writing—review and editing. J.L. performed investigation, writing—review and editing. S.-W.K. performed investigation, writing—review and editing. S.K. performed conceptualization, methodology, writing—review and editing, supervision.

Data Availability Statement

Research data are not shared.

Keywords

bovine bone minerals, critical defects, moldable bones, preclinical trials, regeneration

Received: December 13, 2022
Revised: February 26, 2023
Published online:

[1] Z. Luo, J. Che, L. Sun, L. Yang, Y. Zu, H. Wang, Y. Zhao, *Eng. Regen.* **2021**, *2*, 257.
[2] Y. Zhu, B. Kong, R. Liu, Y. Zhao, *Smart Med.* **2022**, *1*, 20220006.
[3] Z. Fu, Y. Zhuang, J. Cui, R. Sheng, H. Tomás, J. Rodrigues, B. Zhao, X. Wang, K. Lin, *Eng. Regen.* **2022**, *3*, 163.
[4] P. Habibovic, *Tissue Eng. Part A.* **2017**, *23*, 1295.
[5] M. R. Senra, M. de Fátima Vieira Marques, *J. Compos. Sci.* **2020**, *4*, 191.
[6] R. Zhao, R. Yang, P. R. Cooper, Z. Khurshid, A. Shavandi, J. Ratnayake, *Molecules* **2021**, *26*, 3007.
[7] P. L. Carlisle, T. Guda, D. T. Silliman, R. G. Hale, P. R. Brown Baer, *J. Korean Assoc. Oral Maxillofac. Surg.* **2019**, *45*, 97.
[8] J. L. Munante-Cardenas, S. Olate, L. Asprino, J. R. de Albergaria Barbosa, M. de Moraes, R. W. Moreira, *J. Craniofac. Surg.* **2011**, *22*, 1251.
[9] S. Mukhopadhyay, S. Galui, R. Biswas, S. Saha, S. Sarkar, *J. Korean Assoc. Oral Maxillofac. Surg.* **2020**, *46*, 183.
[10] M. R. Iaquinta, E. Mazzoni, I. Bononi, J. C. Rotondo, C. Mazziotta, M. Montesi, S. Sprio, A. Tampieri, M. Tognon, F. Martini, *Front. Cell. Dev. Biol.* **2019**, *7*, 268.
[11] S. Najeeb, M. S. Zafar, Z. Khurshid, S. Zohaib, K. Almas, *Nutrients* **2016**, *8*, 530.
[12] P. L. Carlisle, T. Guda, D. T. Silliman, W. Lien, R. G. Hale, P. R. Brown Baer, *J. Korean Assoc. Oral Maxillofac. Surg.* **2016**, *42*, 20.
[13] C. Vaquette, J. Mitchell, S. Ivanovski, *Front. Bioeng. Biotechnol.* **2021**, *9*, 798393.
[14] G. G. Choi, S. Kim, M. M. Rahman, J. H. Oh, Y. S. Cho, H. J. Shin, *PLoS ONE* **2021**, *16*, e0235454.
[15] D. R. Hunt, S. A. Jovanovic, U. M. Wikesjö, J. M. Wozney, G. W. Bernard, *J. Periodontol.* **2001**, *75*, 651.
[16] J. Charan, N. D. Kantharia, *J. Pharmacol. Pharmacother.* **2013**, *4*, 303.
[17] R. L. Barrack, M. Santman, L. P. Patron, S. L. Salkeld, T. S. Whitecloud, *Clin. Orthop. Relat. Res.* **2000**, *381*, 47.
[18] Y.-K. Sun, J.-K. Cha, D. S. Thoma, S.-R. Yoon, J.-S. Lee, S.-H. Choi, U.-W. Jung, *BioMed. Res. Int.* **2018**, *2018*, 5437361.
[19] L. M. Wancket, *Vet. Pathol.* **2015**, *52*, 842.
[20] A. D. Talley, K. N. Kalpakci, D. A. Shimko, K. J. Zienkiewicz, D. L. Cochran, S. A. Guelcher, *Tissue Eng. Part A.* **2016**, *22*, 469.

[21] J. Anzai, T. Nagayasu Tanaka, A. Terashima, T. Asano, S. Yamada, T. Nozaki, *PLoS ONE* **2016**, *11*, e0158485.
[22] J. S. Lee, U. M. E. Wikesjö, U. W. Jung, S. H. Choi, S. Pippig, M. Siedler, C. K. Kim, *J. Clin. Periodontol.* **2010**, *37*, 382.
[23] S. A. Park, H. J. Lee, K. S. Kim, S. J. Lee, J. T. Lee, S. Y. Kim, N. H. Chang, S. Y. Park, *Materials* **2018**, *11*, 238.
[24] Y. D. Rakhmatia, Y. Ayukawa, Y. Jinno, A. Furuhashi, K. Koyano, *Odontology* **2017**, *105*, 408.
[25] E. J. Harvey, P. V. Giannoudis, P. A. Martineau, J. L. Lansdowne, R. Dimitriou, T. F. Moriarty, R. G. Richards, *J. Orthop. Trauma* **2011**, *25*, 488.
[26] J.-Y. Huh, B.-H. Choi, B.-Y. Kim, S.-H. Lee, S.-J. Zhu, J.-H. Jung, *Oral. Surg. Oral. Med. Oral. Pathol. Oral. Radiol. Endod.* **2005**, *100*, 296.
[27] O. H. Sandberg, P. Aspenberg, *Acta. Orthop.* **2016**, *87*, 459.
[28] M. Maglio, F. Salamanna, S. Brogini, V. Borsari, S. Pagani, N. N. Aldini, G. Giavaresi, M. Fini, *BioMed. Res. Int.* **2020**, *2020*, e1804630.